Stoichiometry and Packing Structure of Poly(Lactic Acid) Stereocomplex As Revealed by Solid-State NMR and ^{13}C Isotope Labeling

Wenxuan Zhou,[†,1] Kun Wang, [†,1] Shijun Wang, [†] Shichen Yuan, [†] Wei Chen, [‖] Takashi Konishi,[‡, †] and Toshikazu Miyoshi [†,*]

† Department of Polymer Science, The University of Akron, Akron, Ohio 44325-3909, United States. ‖ State Key Lab of Pollution Control and Resource Reuse Study College of Environmental Science and Engineering, Tongji University, Shanghai 200092, China. ‡ Graduate School of Human and Environmental Studies, Kyoto University, Kyoto 606-8501, Japan.

Keywords; Poly(Lactide), Stereocomplex, Packing Structure, Solid-State NMR, Double Quantum, Isotope labeling

ABSTRACT: Poly(L-lactic Acid) (L)/poly(D-lactic Acid) (D) blends form a stereocomplex (SC) at a mixing ratio of 7/3-3/7. The stoichiometry and packing structure of L/D in the SC are controversial topics because the SC is semicrystalline and because the enantiomeric pair has the same chemical structure. In this study, both the stoichiometry and packing structure of 33 % ^{13}C CH_3-labeled (*l*) L/nonlabeled D blends at mixing ratios of 7/3 - 3/7 were investigated by using solid-state (SS) NMR. The ^{13}C CO signals in natural abundance provided the fractions of the SC (Φ_{SC}), α, and amorphous regions of *l*-L/D blends. Moreover, the 33 % $^{13}CH_3$-labeled signals could determine the fraction of only *l*-L in the SC (Φ_L) and amorphous region. These two data sets allowed us to determine the stoichiometry of *l*-L/D in the SC ($\Phi_{L\text{-}SC}/\Phi_{D\text{-}SC}$) to be 1/1. ^{13}C-^{13}C double-quantum (DQ) buildup curves of *l*-L in the SC followed one universal curve even at different mixing ratios. Comparison of the experimental and simulated DQ curves led to the conclusion that all SC crystals adopt a regular packing structure at varied mixing ratios.

Stereoregular polymers having a chiral center in the backbone can adopt either right- or left-handed helices. For example, poly(L-Lactic Acid) (L) and poly(D-Lactic Acid) (D) helices adopt left (*L*) and right handedness (*R*), respectively. In 1987, Ikada *et al* found that i) L/D enantiomeric crystals obtained from precipitation-induced stereocomplex (SC) crystallization had a much higher melting temperature (T_m) (~ 220 °C) than L (or D) homo α crystals (ca. 180 °C), ii) SC formation occurred at asymmetric blending ratios, iii) the melting temperature was almost independent of the mixing ratio, and iv) the SC fraction (Φ_{SC}) was maximized at a 1/1 blending ratio[1] The excellent thermal properties of SCs have generated attention to their structure and structural formation process.[1-10] Moreover, L/D chains with a 1:1 ratio were assumed to form SC crystals (Case 1). In 1997, Cartier *et al* proposed a more plausible revised model, R_{3c} ($R_{\bar{3}c}$), where three 3_1 L helices pack with three D helices by paring L (*L*) and D (*R*) helices in a trigonal unit cell with $a = b = 1.498$ nm, $c = 0.87$ nm, $\alpha = \beta = 90$ ° and $\gamma = 120$ ° (Figure 1c).[10] R_{3C} allows only one orientation of either u or d, while $R_{\bar{3}c}$ allows statistical disorder of the up- and downward orientations at each site.

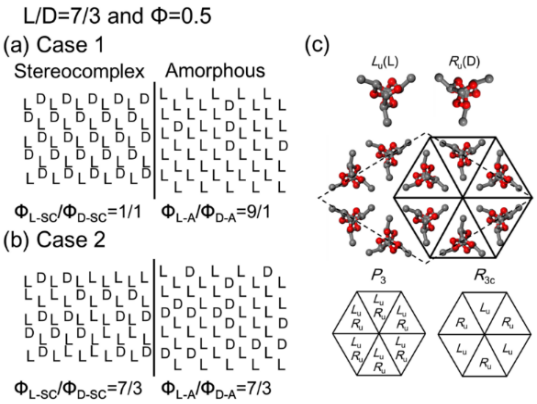

Figure 1. Schematic illustrations of (a) stoichiometry of L/D in Case 1 where ($\Phi_{L\text{-}SC}/\Phi_{D\text{-}SC}$)= 1/1 in the SC and 9/1 in the amorphous region ($\Phi_{L\text{-}A}/\Phi_{D\text{-}A}$) and (b) in Case 2 where L/D = 7/3 in both the SC and the amorphous region at a mixing ratio of L/D = 7/3 and Φ_{SC}= 0.5. (c) Schematic illustrations of a crystal unit cell of R_{3c}[10] (dashed line) and hexagonal packing in the R_{3c} and P_3 models.[11,12]

In 2017, Tashiro *et al* reinvestigated fiber X-ray diffraction (XRD) patterns of SC melt-grown crystals prepared at mixing ratios of L/D= 7/3 - 3/7 and proposed a heterogeneous packing structure, i.e., the P_3 model (Case 2),[11] where either R_u or L_d occupies one site with the probability determined by the mixing ratio and the neighboring site is occupied by either R_d or L_u with the same probability (Figure 1c). However, differences between simulated XRD patterns based on the P_3 and R_{3c} models were very small. Therefore, a different approach that can sensitively distinguish the former case from the latter one is necessary to conclude the packing structure.

An alternative strategy for indirectly checking the packing structure is determination of the stoichiometry of L/D in the SC ($\Phi_{L\text{-}SC}/\Phi_{D\text{-}SC}$). Here, the stoichiometry in Cases 1 and 2 was considered under the assumption of a mixing ratio of L/D = 7/3 and Φ_{SC}= 0.5. In the former case, $\Phi_{L\text{-}SC}/\Phi_{D\text{-}SC}$ and the stoichiometry of

L/D in the amorphous region ($\Phi_{L\text{-}A}/\Phi_{D\text{-}A}$) were expected to be 1/1 and 9/1, respectively (Figure 1a). On the other hand, the stoichiometry of L/D in both regions was 7/3 in the latter case (Figure 1b). To the best our knowledge, there is no research on the stoichiometry in SCs except for one recent work.[12] By applying vibrational circular dichroism (VCD)/IR spectroscopy, Tashiro *et al* suggested the presence of excess L or D species in the SC (Case 2).[12] However, even VCD/IR spectroscopy could not determine $\Phi_{L\text{-}SC}/\Phi_{D\text{-}SC}$ or $\Phi_{L\text{-}A}/\Phi_{D\text{-}A}$.

Solid-state (SS) NMR is a powerful tool to investigate the local structures and dynamics of polymers.[13-23] In particular, the local conformation,[15] packing structure,[16] and chain trajectory[17-20] have been successfully investigated in selectively labeled samples by dipolar-based NMR techniques. In this work, the stoichiometry and packing structure of mixed L/D SCs were investigated by using SS-NMR and selectively ^{13}C isotope labeled (*l*) L chains. ^{13}C high-resolution NMR of the CO signal in natural abundance was used to determine the fraction of L/D in the SC (Φ_{SC}) as a function of the mixing ratio.[21-23] ^{13}C 33 % CH_3-labeled *l*-PLLA signal selectively quantified the fraction of L chains in the SC (Φ_L) and amorphous region. Combining NMR signals for different functional groups of the same sample allowed us to absolutely determine the L/D stoichiometry in both the SC and amorphous regions. Next, the packing structure of L chains in the SC was investigated by using ^{13}C-^{13}C double-quantum (DQ) NMR,[24] which detects spatial correlations among multiple ^{13}C-labeled nuclear spins on the basis of the packing structure of ^{13}C-labeled polymers.[16-20] Comparison of experimental and simulated curves elucidated whether the SC forms regularly alternative packing (R_{3c} or $R_{\bar{3}c}$) or randomly heterogeneous packing (P_3).

33 % ^{13}C CH_3-labeled (*l*) PLLA and nonlabeled PDLA with weight average molecular weights, $<M_w>$, of 143k g/mol (PDI= 1.28) and 2.9k g/mol (PDI= 1.09), respectively, were synthesized in this study. Chain length is a very important parameter that significantly affects SC formation.[20] *l*-PLLA and PDLA with weight mixing ratios of 7/3 - 3/7 were dissolved in dichloromethane. Solutions were evaporated at ambient temperature for 2 days under ambient pressure and further dried for 1 day under vacuum. DSC was conducted on the prepared films (Figure S1). Obviously, low (164-169 °C) and high melting peaks (226 °C) corresponding to melting of pre-existing α and SC crystals, respectively were observed.[1] To melt the pre-existing α crystals, all the samples were heat-treated at 200 °C for 5 min. Subsequently, the samples were quenched to 154 °C and annealed for 12h. Then, the samples were rapidly quenched into icy water. Experimental details of both SS-NMR and XRD are described in the supporting information (SI).

Figure 2a and b shows the CO and CH_3 regions of the ^{13}C CPMAS NMR spectra (black lines) of ^{13}C CH_3-labeled *l*-L/nonlabeled D blends at mixing ratios of 7/3, 5/5, and 3/7. Additional NMR data of the SCs at mixing ratios of 6/4 and 4/6 are depicted in Figure S2, and the corresponding XRD patterns are depicted in Figure S3. The samples at L/D= 7/3 and 5/5 showed asymmetric SC signals at 173 ppm along with a broad amorphous peak

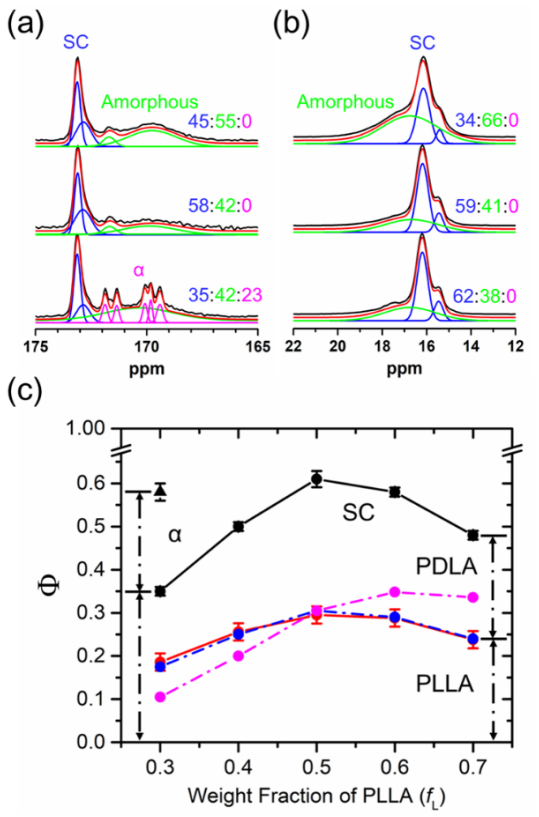

Figure 2. ^{13}C CPMAS NMR experimental and calculated spectra for the (a) CO and (b) CH_3 regions of *l*-L/D blends at mixing ratios of L/D= 7/3, 5/5, and 3/7. (c) Φ_{SC} (black circles), Φ_α (black triangle), and $\Phi_{L\text{-}SC}$ (filled red circle) at f_L = 0.3-0.7 determined by CPMAS NMR lineshape analysis and the fraction of L in the SC in the sample predicted from Cases 1 (blue) and 2 (pink) and Φ_{SC}.

centered at 170 ppm and an additional small peak at 171.6 ppm.[21-23] In previous works, this small signal was similarly observed in L/D blend samples[21-23] and was assigned to the α phase.[21] However, the chemical shift is not consistent with the two α peaks at 171.2 and 171.8 ppm[21-23] in the sample at L/D= 3/7 (bottom of Figure 2a). Additionally, the other three signals at 169 - 170 ppm[21-23] were not observed in the CO signal region of the samples at 7/3 and 5/5. Moreover, the XRD and ^{13}C CH_3 signals of the samples at L/D= 7/3 and 5/5 (see below) did not show characteristic α peaks. Thus, this tiny signal was assigned as part of the amorphous region. The CPMAS NMR signal intensity highly depends on C-H dipolar interactions, which are modulated by molecular dynamics. The T_g of poly(lactic acid) (ca. 60 °C) is relatively higher than the experimental temperature (25 °C). Assuming that the CP efficiencies are the same between the crystalline and amorphous regions, crystallinity could be determined using a conventional CPMAS NMR experiment. Conducting least-squares fitting of Gaussian peaks to the NMR spectra allowed the Φ_{SC} (filled black circle) and α fraction (Φ_α) (black triangle) to be obtained, as plotted in Figure 2c. At L/D =7/3, Φ_{SC} was 0.45. The maximum SC formation was 0.58 at L/D= 5/5. As the content of D species increased further, Φ_{SC} was decreased to 0.35, accompanied by the appearance of α crystals (0.23). A similar trend was also observed in the XRD patterns, as shown in Figure S3.

Figure 2b depicts the ^{13}C CH_3 regions of *l*-L/D in the blends. Theoretically, the 33 % labeling ratio of *l*-L provides a 30-fold higher intensity than the CH_3 signals of D. Therefore, the contribution of D to the apparent CH_3 signals was simply ignored in our analysis. The CH_3 signals in the α phase gave two sharp peaks at 16 and 17 ppm, which were not observed in the CH_3 signal region throughout the whole mixing range. Comparison of the CO and CH_3 signals directly demonstrated that the α crystals formed at L/D= 3/7 originate from excess D species. An asymmetric SC lineshape at 16 ppm and a broad amorphous peak at 17 ppm were clearly observed in all of the compositions.[21-23] At L/D= 7/3, $\Phi_{L\text{-}SC}$ was 0.34, and with increasing D content, $\Phi_{L\text{-}SC}$ increased and reached a maximum of 0.62 at L/D = 3/7.

The $\Phi_{L\text{-}SC}$ in the whole sample (Φ_L) (red filled circle) can be obtained by multiplying $\Phi_{L\text{-}SC}$ by the weight fraction of L in the sample (f_L). Φ_L (filled red circle) as a function of f_L is plotted in Figure 2c. The expected fractions of L in the SC in the sample in Cases 1 (blue filled circle) and 2 (pink) as a function of f_L were calculated by using the expected Φ_L and stoichiometry of L/D in the SC in Cases 1 and 2 and are plotted in Figure 2c. At both edges of f_L= 0.3 and 0.7, significant deviations between the experimental and expected curves for Case 2 can be observed. The whole experimental curve is well consistent with the curve based on Case 1. The fraction of D in the SC in the sample (Φ_D) could be obtained simply by subtracting Φ_L from Φ_{SC}. $\Phi_{L\text{-}SC}/\Phi_{D\text{-}SC}$ was experimentally determined and is provided in Table S1. For example, $\Phi_{L\text{-}SC}/\Phi_{D\text{-}SC}$ was 53/47, 49/51, and 53/47 at f_L = 0.7, 0.5, and 0.3, respectively. Similarly, $\Phi_{L\text{-}A}/\Phi_{D\text{-}A}$ could also be obtained in a similar way and is provided in Table S1. Both data sets convincingly proved that $\Phi_{L\text{-}SC}/\Phi_{D\text{-}SC}$ is 1:1 when the mixing ratio was varied from 7/3 – 3/7 (Case 1).

^{13}C-^{13}C DQ experiments were further conducted on the L/D blend samples to confirm the packing structure of the SC. In the case of the R_{3c} ($R_{\bar{3}c}$) model, the *L* stems are located at three sites in the available hexagons shown in Figure 3a. The atomic coordinates of the CH_3 carbons in the R_{3c} model are the same as those in the $R_{\bar{3}c}$ model. Therefore, DQ NMR of the *l*-L sample cannot distinguish between R_{3c} and $R_{\bar{3}c}$.[20] Thus, our discussions are limited to only the packing structure of either R_{3c} or P_3. In the R_{3c} model,[10] a maximum five-spin system including a reference one at distances less than 7 Å as depicted in Figure 3a was statistically treated in calculations of the ^{13}C-^{13}C DQ buildup curve.[16-20] In our previous work, the atomic coordinates reported by Cartier *et al*[10] were slightly modified and used for chain-folding analysis in SC single crystals.[20] The inter-nuclear distances used in the simulation (3.91 and 5.22 Å) are depicted in Figure 3a. In this study, the same distances

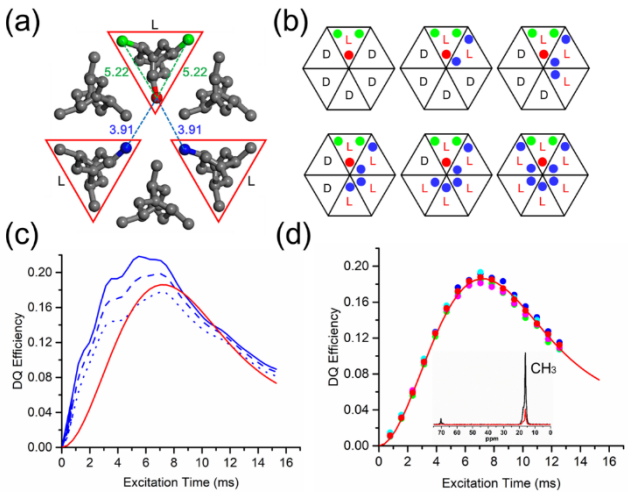

Figure 3. (a) R_{3c} packing model and ^{13}C five spin systems of *l*-L in SC including reference (red) two intrastem (green) and two interstem spins (blue) within 7 Å used in simulations for DQ buildup curve. (b) Six submodels including different L stem numbers and corresponding spin topologies in P_3. (c) Simulated ^{13}C-^{13}C DQ buildup curves on the basis of R_{3C} (red solid) and P_3 models (blue) at mixing ratio of L/D=7/3 (solid), 5/5 (dashed), and 3/7(dotted) with T_2 value of 9.5 ms. (d) ^{13}C CPMAS SQ (black) and DQ (red) NMR spectra for the 33 % *l*-L/D blends at a mixing ratio of L/D= 5/5, with an excitation time of 6.27 ms and experimental DQ buildup curves for *l*-L/D SC signals at L/D mixing ratios of 7/3 (pink filled circle), 6/4 (light blue), 5/5 (blue), 4/6(green), and 3/7 (red) with the simulated curve for R_{3c} model.

used in our previous work[20] were used in the calculations of the DQ buildup curve by applying a spin-spin relaxation time (T_2) of 9.5 ms. The simulated curve is shown as a red curve in Figure 3c (for details, see ref 20). In the P_3 model, *L* stems are randomly located at each site of the six available sites in the hexagon depending on mixing ratio of 7/3- 3/7, as schematically depicted in Figure 3b. Six kinds of submodels including different *L* stem numbers of 1 - 6 at the six available sites were constructed. Each submodel statistically includes several combinations of different stem occupations at the six sites (for details, see Table S2). All possible combinations were statistically considered. At each mixing ratio (7/3, 5/5, and 3/7), one curve was ultimately generated as a result of the weight-averaged DQ curves for all submodels, as illustrated in Figure 3b, where the atomic coordinates of the CH_3 carbons reported by Tashiro *et al*[11] and the same distance limitation (within 7 Å) as the R_{3c} model were applied. The mixing-ratio dependence of the simulated DQ buildup curves of *l*-L stems in the P_3 model can be clearly seen (Figure 3c). All the simulated curves at L/D= 7/3, 5/5, and 3/7 showed a much faster increase at the initial stage and a higher maximum DQ efficiency than the simulated curve for the R_{3c} model. These results originate from the unrealistically short CH_3-CH_3 carbon distances (2.54 Å) between neighboring stems having the same handedness (see Table 2 and Figure 16 in ref 11). Faster buildup curves implied necessity of substantial revisions of the P_3 model by slightly rotating and/or shifting individual stems and/or expanding the unit cell. The atomic-level resolution of DQ NMR allows it to convincingly distinguish between R_{3c} and P_3 proposed by the electron diffraction[10] and XRD[11] patterns. Figure 3d illustrates experimental DQ buildup curves of ^{13}C *l*-L chains in the SC at mixing ratios of L/D = 7/3-3/7. The individual DQ buildup curves were almost identical with each other and could be fit by using the simulated curve based on the R_{3c} model used in Figure 3c. The results clearly indicate that L and D chains alternatively pack with each other and for

the R_{3c} ($R_{\bar{3}c}$) packing structure. The DQ NMR data and CPMAS data obviously proved Case 1.

Another interesting feature is the structural information about excess L or D species. At L/D = 7/3, excess L chains did not crystallize as homo α crystals during cooling process from 160 °C to ambient temperature. On the other hand, excess D chains crystallized under the same cooling conditions. The crystallization of excess chains was related to chain length. At L/D= 7/3, long L chains partially formed a SC with short D chains at T_c = 154 °C. Diffusion of the remaining unpaired L chains was limited due to partial SC formation along the chains and the relaxation process of the long L chains, and thus, the chains stayed close to the SC crystals and could not form pure L domains. On the other hand, at L/D= 3:7, many excess short D chains might be free (no pairing) and, crystallize into the α form during annealing time at 154 °C (Figure S4). Therefore, different chain lengths lead to an asymmetric phase structure of L/D blends.

In summary, the use of SS-NMR and ^{13}C isotope labeling convincingly proved that the pairing of L/D =1:1 forms SCs in R_{3c} ($R_{\bar{3}c}$) at mixing ratios varied from L/D = 7/3-3/7 (Case 1). Interestingly, the current approach can investigate spatial correlations for only one component of an enantiomeric pair. SC formation of L/D highly depends on molecular weights and might be related to the chain-level structures of both L and D in the glassy state. The current approach has potential for investigating the local chain trajectory of enantiomeric systems before and after crystallization.[20] This information will be useful for understanding the structural formation process as well as the packing structure of SCs prepared in solution-[10] and melt-crystallization[11, 12] as a function of molecular weight.

ASSOCIATED CONTENT

Supporting Information. SS-NMR and XRD experimental conditions; XRD, DSC, and CPMAS NMR spectra; stoichiometry of L/D in the SC and amorphous regions; and submodels in the P_3 model. This material is available free of charge via the Internet at http://pubs.acs.org.

AUTHOR INFORMATION

Corresponding Author * miyoshi@uakro.edu

Notes

The authors declare no competing financial interest.

Author Contributions

1These authors contributed equally.

ACKNOWLEDGMENT

This work was financially supported by the National Science Foundation (Grant no. DMR–1708999).

REFERENCES

1. Ikada Y.; Jamshidi, K.; Tsuji, H.; Hyon, S-H. Stereocomplex Formation between Enantiometric Poly(Lactides). *Macromolecules* **1987**, 20, 904–906.
2. Tsuji, H.; Horii, F.; Hyon, S. H.; Ikada, Y. Stereocomplex Formation between Enantiomeric Poly(1actic acid)s. 2. Stereocomplex Formation in Concentrated Solutions. *Macromolecules* **1991**, *24*, 2719−2724.
3. Tsuji, H.; Ikada, Y. Stereocomplex Formation between Enantiomeric Poly(1actic acid)s. 9. Stereocomplexation from the Melt. *Macromolecules* **1993**, *26*, 6918−6926.
4. Brochu, S.; Prud'homme, R. E.; Barakat, I.; Jérome, R. Stereocomplexation and Morphology of Polylactides. *Macromolecules* **1995**, *28*, 5230−5239.
5. Zhang, J.; Sato, H.; Tsuji, H.; Noda, I.; Ozaki Y. Infrared Spectroscopic Study of CH3-OC Interaction during Poly(L-Lactid)/Poly(D-Lactide) Stereocommplex Formation. *Macromolecules* **2005**, *38*, 1822–1828.
6. Yang, C-F.; Huang, Y-F.; Ruan, J.; Su A-C. Extensive Development of Precursory Helical Pairs Prior to Formation of Stereocomplex Crystals in Racemic Polylactide Melt Mixture. *Macromolecules* **2012**, *45*, 872–878.
7. Okihara, T.; Tsuji, M.; Kawaguchi, A.; Katayama, K.; Tsuji, H. Hyon, S.H.; Ikada, Y. Crystal Structure of Strereocomplex of Poly(L-Lactide) and Poly(D-Lactide). *J. Macromol. Sci., Part B: Phys*. **1991**, 30, 119-140.
8. Brizzolara, D.; Cantow, H. J.; Diederichs, K.; Keller, E.; Domb A. J. Mechanism of the Stereocomplex Formation between Enantiomeric Poly(lactide)s. *Macromolecules* **1996**, 29, 191−197.
9. Tsuji, H. Poly(Lactic Acid) Stereocomplexes: A Progress of Decade. *Adv. Drug. Delivery Rev*. 2016, 107, 97−135.
10. Cartier, L.; Okihara, T.; Lotz, B.; Trianglular Polymer Single Crystals: Sterocomplexes Twins, and Frustrated Structures. *Macromolecules* **1997**, *30*, 6313–6322.
11. Tashiro, K.; Kouno N.; Wang, H.; Tsuji H. Crystal Structure of Poly(Lactic Acid) Stereocomplex: Random Packing Model of PDLA and PLLA Chains As Studied by X-ray Diffraction Analysis. *Macromolecules* **2017**, *50*, 8048–8065.
12. Tashiro K.; Wang, H.; Kouno N.; Koshobu, J.; Watanabe K. Conformation of the X-ray Analyzed Heterogeneous Distribution of the PDLA and PLLA Chain Stems in the Crystal Lattice of Poly(Lactic Acid) Complex on the Basis of the Vibrational Circular Dichroism IR Spectral Measurement. *Macromolecules* **2017**, *50*, 8066–8071.
13. Spiess, H. W. 50th Anniversary Perspective: The Importance of NMR Spectroscopy to Macromolecular Science. *Macromolecules* **2017**, *50*, 1761-1777.
14. Hansen M. R.; Graf, R.; Spiess, H. W. Interplay of Structure and Dynamics in Functional Macromolecular and Supramolecular Systems AS Revealed by Magnetic Resonance Spectroscopy. *Chem. Rev*. **2016**, *116*, 1271-1308.
15. Schmidt-Rohr, K.; Hu, W.; Zumbulyadis, N.; Elucidation of the Chain Conformation in a Glassy Polyester, PET, by Two-Dimensional NMR. *Science* **1998**, *280*, 714-717.
16. Yuan, S.; Li, Z.; Kang, J.; Hong, Y.; Kamimura, A.; Otsubo, A.; Miyoshi, T. Determination of Local Packing Structure of Mesomorphic Form of Isotactic Polypropylene by Solid-State NMR. *ACS Macro Lett*. **2015**, *4*, 143–146.
17. Hong, Y.-l.; Chen, W.; Yuan, S.; Kang J.; Miyoshi T. Chain Trajectory of Semicrystalline Polymers As Revealed by Solid-State NMR Spectroscopy. *ACS Macro Lett*. **2016**, *5*, 355–358.
18. Hong, Y.-l.; Miyoshi, T. Chain-Folding Structure of a Semicrystalline Polymer in Bulk Crystals Determined by ^{13}C-^{13}C Double Quantum NMR. *ACS Macro. Lett*. **2013**, *2*, 501–505.

19. Wang, S.; Yuan, S.; Chen. W.; He, Q.; Hong, Y.-l.; Miyoshi, T. Solid-State NMR Study of the Chain Trajectory and Crystallization Mechanism of Poly(L-Lactic Acid) in Dilute Solution. *Macromolecules* **2017**, 50, 6404–6414.

20. Chen W.; Wang S. Zhang W., Hong Y-l., Miyoshi T. Molecular Structural Basis for Stereocomplex Formation of Poly(Lactide)s in Dilute Solution. *ACS Macro Lett*. **2015**, *4*, 1264–1267.

21. Tsuji, H.; Horii, F.; Nakagawa, M.; Ikada, Y.; Odani, H.; Kitamaru R. Stereocomplex formation between enantiomeric poly(lactic acid)s. 7. Phase structure of the stereocomplex crystallized from a dilute acetonitrile solution as studied by high-resolution solid-state carbon-13 NMR spectroscopy. *Macromolecules* **1992**, *25*, 4114–4118.

22. Chen, W.; Zhou, W.; Makita, Y.; Wang, S.; Yuan, S.; Konishi, T.; Miyoshi, T. Characterization of the Slow Molecular Dynamics of Poly(l-Lactic Acid) in α and α' Phases, in a Glassy State, and in a Complex with Poly(d-Lactic Acid) by Solid-State NMR. *Macromol. Chem. Phys.* **2018**, 219, 1700451.

23. Chen, W.; Reichert. D.; Miyoshi, T. Short-Range Correlation of Successive Helical Jump Motions of Poly(L-Lactic Acid) Chains in the α Phase as Revealed by Solid-State NMR. *J. Phys. Chem. B* **2015**, *119*, 4552–4563.

24. Hohwy, M.; Jakobsen, H. J.; Eden, M.; Levitt, M. H.; Nielsen, N. C. Broadband dipolar recoupling in the nuclear magnetic resonance of rotating solids: A compensated C7 pulse sequence. *J. Chem. Phys*. **1998**, *108*, 2686–2694.

Stoichiometry and Packing Structure of Poly(Lactic Acid) Stereocomplex As Revealed by Solid-State NMR and ^{13}C Isotope Labeling

Wenxuan Zhou, Kun Wang, Shijun Wang, Shichen Yuan, Wei Chen, Takashi Konishi, and Toshikazu Miyoshi